

Boundaries of Subcritical Coulomb Impurity Region in Gapped Graphene

B. S. Kandemir and A. Mogulkoc
*Department of Physics, Faculty of Sciences,
Ankara University, 06100
Tandoğan, Ankara, Turkey*
(Dated: September 15, 2021)

The electronic energy spectrum of graphene electron subjected to a homogeneous magnetic field in the presence of a charged Coulomb impurity is studied analytically within two-dimensional Dirac-Weyl picture by using variational approach. The variational scheme we used is just based on utilizing the exact eigenstates of two-dimensional Dirac fermion in the presence of a uniform magnetic field as a basis for determining analytical energy eigenvalues in the presence of an attractive/repulsive charged Coulomb impurity. This approach allows us to determine under which conditions bound state solutions can or can not exist in gapped graphene in the presence of magnetic field. In addition, the effects of uniform magnetic field on the boundaries of subcritical Coulomb impurity region in the massless limit are also analyzed. Our analytical results show that the critical impurity strength decreases with increasing gap/mass parameter, and also that it increases with increasing magnetic field strength. In the massless limit, we investigate that the critical Coulomb coupling strength is independent of magnetic field, and its upper value for the ground-state energy is 0.752.

PACS numbers: 81.05.Uw,73.63.Fg,73.63.-b,71.55.-i

Since the discovery of graphene¹, strictly two-dimensional (2D) carbon system with hexagonal lattice structure, a great deal of both experimental and theoretical research efforts has been achieved to identify the electronic structures of graphene and graphene based nanostructures such as graphene dots and graphene nanoribbons². In fact, from the theoretical point of view, after Wallace's work³, Semenoff⁴ was the first to construct the relativistic 2+1 dimensional electrodynamics analogue of tight-binding model of electrons in a 2D hexagonal lattice. In other words, he investigated that, in the long-wave length (continuum) limit, the low-energy electronic structure of this model exhibits linearly dispersing massless fermionic quasi particles around the degeneracy points obeying to 2+1 Dirac-Weyl Hamiltonian. As a consequence, all the single particle low-energy physics of graphene is believed to be well simulated by the Dirac-Weyl equation.

Due to their relevance for the transport properties, impurity effects are, at present, at the center of both theoretical and experimental investigations in graphene physics⁵⁻¹². There are non-negligible effects especially on the electronic properties of graphene based devices, since the Dirac points of undoped graphene which are very sensitive to such effects¹³. Additionally, a recent experiment¹⁴ performed by depositing potassium atoms onto undoped graphene addresses charged Coulomb like behavior. Moreover, it is shown that a pronounced asymmetry occurs in transport cross-section depending upon $Z \rightarrow -Z$ for the Coulomb scattering¹⁵⁻¹⁸, and it is also believed that the long-range charged Coulomb impurity limit the mobility of graphene.^{14,19}

From the quantum electrodynamical (QED) point of view, it is well-known that the interactions between the charged particles are associated by the exchange of virtual photons. These interactions are represented by a fermionic Coulomb potential which is identified with its perturbative expansion in powers of the fine structure $\alpha = e^2/\hbar c = 1/137$. However, it is broken down in the case of superheavy nuclei, atoms or quasi-molecules where α is of order of unity²⁰. This hypothetical regime with $Z\alpha > 1$ which requires a non-perturbative treatment (due to difficulties of convergence of expansions) has been of academic interest in the past. However, due to the fact that the effective coupling constant of graphene is at order of $\alpha = e^2/\varepsilon\hbar v_F \sim 1$ for conventional SiO₂ substrate^{6-8,15,16}, condensed matter analog of this regime is of experimental interest, and it is now at the center of theoretical investigations. In particular, "mass" or energy gap in graphene is frequently interpreted as being related to chiral symmetry breaking of 2D massless Dirac-Weyl fermions induced by substrate²¹, spin-orbit coupling²², and by boundary conditions²³. Since this enables one to tune a gap by just adjusting the external parameters of graphene, it is of particular interest itself.

In the present paper, we investigate analytically the effects of a Coulomb impurity with effective charge Ze onto the energy spectrum of 2D massive fermions, i.e., gapped graphene, with a uniform magnetic field perpendicular to the graphene plane. In other words, we analyze the effects of uniform magnetic field onto the graphene electron with impurity, and hence we determine the boundaries of subcritical regime. As mentioned above, due to both strong coupling and long-range characters of the Coulomb impurities in graphene, these effects can not be addressed by conventional perturbative techniques. Therefore, we suggest a variational approach to account for such effects, induced by the impurity.

The Dirac Hamiltonian with electromagnetic potentials that we describe the motion of an electron and a hole in 2D graphene subjected to a constant uniform magnetic field, perpendicular to graphene plane, can be written in the

form

$$H = \hbar v_F \boldsymbol{\alpha} \cdot \left(-i\partial_\mu + \frac{e}{\hbar c} \mathbf{A} \right) + \beta m v_F^2 - e A_0(r), \quad (1)$$

where A_0 and A_μ are the time and space components of the four-vector potential (A_0, A_μ) , due to impurity $A_0 = Ze/\epsilon r$ and static uniform magnetic field with $\mathbf{A} = B(-y, x)/2$, respectively. Here, while $Z > 0$ refers to the attractive impurity potential that binds electrons to impurity and repels holes, or vice versa if $Z < 0$. In Eq. (1), we have used the Dirac-Pauli representation of Dirac matrices, $\boldsymbol{\alpha}$ and $\boldsymbol{\beta}$, each of which are written in two by two-block form. Using two component spinor representation as $\Psi^\dagger = (\phi^* \ \chi^*)$, we see that each component of the eigenvalue equation $H\Psi = E\Psi$ satisfies the following coupled first order equation:

$$\begin{aligned} \boldsymbol{\sigma} \cdot \left(-i\partial_\mu + \frac{e}{\hbar c} A_\mu \right) \chi + [M_0 - \bar{E} - e\bar{A}_0(r)] \phi &= 0 \\ \boldsymbol{\sigma} \cdot \left(-i\partial_\mu + \frac{e}{\hbar c} A_\mu \right) \phi - [M_0 + \bar{E} + e\bar{A}_0(r)] \chi &= 0, \end{aligned} \quad (2)$$

where we write energy, coupling strength and "mass" terms in units of $\hbar v_F$, as $\bar{E} = E/\hbar v_F$, $\bar{A}_0(r) = Ze/\hbar v_F r$, and $M_0 = m v_F/\hbar$, respectively. From our knowledge on planar relativistic and non-relativistic electron systems in the presence of both Coulomb and magnetic field, it is not possible to find exact analytical solutions^{24,25} of Eq. (2) due to having hidden sl_2 algebraic structure²⁶.

Decoupling Eq. (2) in the absence of impurity potential one can easily see that the upper component of Ψ , i.e., ϕ , should satisfy the second order equation

$$\left[-\frac{\partial^2}{\partial \rho^2} - \frac{1}{\rho} \frac{\partial}{\partial \rho} - \frac{1}{\rho^2} \frac{\partial^2}{\partial \varphi^2} - i \frac{eB}{\hbar c} \frac{\partial}{\partial \varphi} + \frac{eB}{\hbar c} \sigma_3 + \left(\frac{eB}{2\hbar c} \right)^2 \rho^2 + (M_0^2 - \bar{E}^2) \right] \phi = 0, \quad (3)$$

whose solutions can then be written in terms of Laguerre polynomials²⁷.

$$\phi_{\nu m, s}(\rho, \varphi) = \left(\sqrt{\frac{eB}{2\hbar c}} \rho \right)^{|m|} e^{im\varphi} e^{-eB\rho^2/4\hbar c} L_\nu^{|m|} \left(\frac{eB}{2\hbar c} \rho^2 \right), \quad (4)$$

provided that the energy quantization condition

$$[4\nu + 2(|m| + 1) + 2(s + m)] \frac{eB}{2\hbar c} = \bar{E}^2 - M_0^2, \quad (5)$$

is fulfilled. It is obvious that Eq. (3) yields infinitely degenerate energy eigenvalues $\bar{E}_n^\pm = \pm [M_0^2 + (2neB/\hbar c)]^{1/2}$ with $n = \nu + [(|m| + m + s + 1)/2]$. Inserting Eq. (4) into Eq. (2), the other component of the spinor can explicitly be determined. Therefore, to the positive energy spinors in the absence of impurity potential, we can write the complete and orthonormalized solutions of Eq. (1) for $s = +1$ and $s = -1$ cases as

$$\Psi_{\nu m, +1}^+(\rho, \varphi) = \frac{1}{\sqrt{\pi}} [N_{\nu m}^+(M_0, B)]^{1/2} \gamma^{|m|+1} \rho^{|m|} \exp(im\varphi) \exp(-\gamma^2 \rho^2/2) \begin{bmatrix} \mathbb{L}_{\nu m, +1}^{1+}(\gamma\rho) \\ 0 \\ 0 \\ \mathbb{L}_{\nu m, +1}^{2+}(\gamma\rho) \end{bmatrix} \quad (6)$$

and

$$\Psi_{\nu m, -1}^+(\rho, \varphi) = \frac{1}{\sqrt{\pi}} [N_{\nu m}^+(M_0, B)]^{1/2} \gamma^{|m|+1} \rho^{|m|} \exp(im\varphi) \exp(-\gamma^2 \rho^2/2) \begin{bmatrix} 0 \\ \mathbb{L}_{\nu m, -1}^{1+}(\gamma\rho) \\ \mathbb{L}_{\nu m, -1}^{2+}(\gamma\rho) \\ 0 \end{bmatrix}, \quad (7)$$

respectively, with the abbreviations

$$\begin{aligned} \mathbb{L}_{\nu m, +1}^{2+}(\gamma\rho) &= \frac{i\gamma\rho \exp(+i\varphi)}{\Gamma(M_0, n)} \begin{cases} L_\nu^{|m|+1}(\gamma^2\rho^2) & m \geq 0 \\ -\frac{\nu+1}{\gamma^2\rho^2} L_{\nu+1}^{|m|-1}(\gamma^2\rho^2) & m < 0 \end{cases} \\ \mathbb{L}_{\nu m, -1}^{2+}(\gamma\rho) &= \frac{i\gamma\rho \exp(-i\varphi)}{\Gamma(M_0, n)} \begin{cases} -\frac{\nu+|m|}{\gamma^2\rho^2} L_\nu^{|m|-1}(\gamma^2\rho^2) & m \geq 0 \\ L_{\nu-1}^{|m|+1}(\gamma^2\rho^2) & m < 0 \end{cases}, \end{aligned}$$

and $\mathbb{L}_{\nu m, +1}^{1+}(\gamma\rho) = \mathbb{L}_{\nu m, -1}^{1+}(\gamma\rho) = L_{\nu}^{|m|}(\gamma^2\rho^2)$, where $L_{\nu}^{|m|}$ are the well-known associated Laguerre polynomials. In Eq. (6) and Eq. (7), we have also defined

$$N_{\nu m}^+(M_0, B) = \frac{\nu!}{(\nu + |m|)!} \frac{M_0 + [M_0^2 + (2n/\ell^2)]^{1/2}}{2[M_0^2 + (2n/\ell^2)]^{1/2}},$$

and

$$\Gamma(M_0, n) = \frac{\ell}{\sqrt{2}} \left\{ M_0 + [M_0^2 + (2n/\ell^2)]^{1/2} \right\},$$

where $\gamma^2 = eB/2\hbar c$, and ℓ is the magnetic confinement length given by $\ell = \sqrt{\hbar c/eB}$. Analogously, one can follow the same treatment for the negative energy spinors.

At this work, we suggest the states given by Eq. (6) and Eq. (7) as the trial states for the whole system, i.e., 2D Dirac equation with charged Coulomb impurity given by Eq. (2). Therefore, for the expectation value of H given by Eq. (1), we obtain

$$\overline{E}_{nms}^{\mp}(\gamma) = \int d^2\mathbf{r} \Psi_{\nu m, \mp 1}^{\mp \dagger}(\gamma) \left[\boldsymbol{\alpha} \cdot \left(-i\partial_{\mu} + \frac{e}{\hbar c} A_{\mu} \right) + \beta M_0 - \tilde{A}_0(r) \right] \Psi_{\nu m, \mp 1}^{\mp}(\gamma) \quad (8)$$

where $\tilde{A}_0(r) = Z\alpha/r$, and α is given by $\alpha = e^2/\varepsilon\hbar v_F$. By using first Eq. (6) together with Eq. (7) in Eq. (8), and then performing the necessary integrals²⁸, the total variational energy $\overline{E}_{nms}^{\pm}(\gamma)$ of the whole system can finally be written in the form

$$\overline{E}_{nms}^{\mp}(\gamma) = \left[1 + \frac{n}{\Gamma^2(M_0, n)} \right]^{-1} \left\{ M_0 \left[1 - \frac{n}{\Gamma^2(M_0, n)} \right] + \left[\frac{2n}{\Gamma(M_0, n)} - Z\alpha \mathbb{M}_{\nu m, s}^{\mp} \right] \gamma + \frac{n}{\ell^2 \Gamma(M_0, n)} \frac{1}{\gamma} \right\}, \quad (9)$$

where we have defined

$$\mathbb{M}_{\nu m, s}^{\mp} = \mathbb{F}_{\nu m, s}^{\mp} + \frac{1}{\Gamma^2(M_0, n)} \mathbb{G}_{\nu m, s}^{\mp, \alpha}, \quad (10)$$

with

$$\mathbb{F}_{\nu m, s}^{\mp} = \frac{\nu!}{(\nu + |m|)!} \int_0^{\infty} dr r^{|m|-1/2} \exp(-r) \left| L_{\nu}^{|m|}(r) \right|^2,$$

$$\mathbb{G}_{\nu m, s}^{\mp, \alpha} = \frac{\nu!}{(\nu + |m|)!} \int_0^{\infty} dr r^{|m|-1/2} \exp(-r) \begin{cases} r \left| L_{\nu+\alpha}^{|m|+1}(r) \right|^2 & \alpha = \begin{cases} 0 & \text{if } m \geq 0 \text{ and } s = +1 \\ -1 & \text{if } m < 0 \text{ and } s = -1 \end{cases} \\ n^2 r^{-1} \left| L_{\nu+\alpha}^{|m|-1}(r) \right|^2 & \alpha = \begin{cases} 0 & \text{if } m \geq 0 \text{ and } s = -1 \\ +1 & \text{if } m < 0 \text{ and } s = +1 \end{cases} \end{cases}.$$

Minimizing Eq. (9) with respect to variational parameter γ , we obtain

$$\gamma = \mp \left\{ \frac{n}{\ell^2 \Gamma(M_0, n)} / \left[\frac{2n}{\Gamma(M_0, n)} - Z\alpha \mathbb{M}_{\nu m, s}^{\mp} \right] \right\}^{1/2}. \quad (11)$$

where we restrict ourselves to the physical positive sign of the variational parameter, due to the sign convention we employed in the normalization^{29,30}. Here, it should also be noted that, in the literature, different sign conventions may be chosen, however some of them may introduce artificial difficulties, especially, in the massless limit (Ref. 29 for a detailed discussion). Therefore, by labeling the electron and hole states $\lambda = +1$ and $\lambda = -1$, respectively, we obtain an analytical result for the whole energy spectrum of the system with Coulomb impurity potential as

$$\overline{E}_n^{\lambda} = \lambda \left(M_0^2 + \frac{2n}{\ell^2} \right)^{-1/2} \left\{ M_0^2 + \frac{2n}{\ell^2} [1 - \mathbb{H}(Z, M_0)]^{1/2} \right\}, \quad (12)$$

with

$$\mathbb{H}(Z, M_0) = \lambda \frac{Z \alpha \mathbb{M}_{\nu m, s}^{\mp}}{2\sqrt{2}} \frac{\ell}{n} \left(M_0 + \sqrt{M_0^2 + \frac{2n}{\ell^2}} \right),$$

for all values of Z and M_0 if and only if $\mathbb{H}(Z, M_0) \leq 1$, which implies the condition

$$(Z\alpha)_{cr} \equiv \bar{Z}_{cr}(M_0, B) = \frac{2\sqrt{2}n/\ell}{\lambda \mathbb{M}_{\nu m, s}^{\mp} \left[M_0 + \sqrt{M_0^2 + 2n/\ell^2} \right]} \quad (13)$$

should be satisfied in order that there might exist oscillator like discrete energy spectrum. Otherwise, Eq. (12) becomes imaginary. In $\mathbb{H}(Z, M_0) = 0$ limit, Eq. (12) becomes $\bar{E}_n^{\pm} = \pm \sqrt{M_0^2 + 2n/\ell^2}$. Thus, we recover the usual Landau picture of 2D Dirac equation with mass.

It should be noted that $\bar{E}_n^{(\pm)}$ given by Eq. (12) depends strongly on the sign of \bar{Z} , i.e., it is asymmetric with respect to reverse of \bar{Z} , due to the fact that, in the presence of a uniform magnetic field, electron (hole) in a attractive impurity potential ($\bar{Z} > 0$, ($\bar{Z} < 0$)) does not have the same energies as electrons (holes) in a repulsive impurity potential ($\bar{Z} < 0$, ($\bar{Z} > 0$)). This is apparent from FIG. 1 (a) and (b) where the evolution of the ground state energy, $\bar{E}_1^{(\pm)}$ of massless graphene electron(hole) in the magnetic field is shown for (a) various values of $\bar{Z} > 0$, and (b) for various values of $\bar{Z} < 0$. As is seen from the figure, when \bar{Z} approaches to $\pm \bar{Z}_{cr}$, $\bar{E}_1^{(\pm)}$ is dramatically reduced, and it vanishes at $\bar{Z} = \pm \bar{Z}_{cr}$. It can be easily seen from Eq. (13) that, in the case of massless graphene, i.e., $M_0 = 0$, this critical value of \bar{Z} , i.e., \bar{Z}_{cr} is given by

$$\bar{Z}_{cr}(0, B) = \pm \frac{2}{\sqrt{n}} \frac{1}{\mathbb{M}_{\nu m, s}^{\mp} |_{M_0=0}} \quad (14)$$

which is independent of ℓ , i.e., of B , and it leads to $\bar{Z}_{cr} = 4/3\sqrt{\pi} = 0.752$ for the ground-state of the system, i.e., for $n = 1$ corresponding to $(\nu, m, s) = (0, 1, -1)$, and $(0, 0, +1)$. In fact, it is well-known that, in the absence of magnetic field, this critical value is equal to $0.5^{7,16}$ for the massive case. This difference arises from the use of oscillator states as trial states in our problem to obtain the dependence of critical value of \bar{Z} on magnetic field. Therefore, it is obvious that our analytical results are valid for high magnetic field regime.

In the presence of a gap/"mass" term, as shown in FIG. 2, the picture is quite different depending on the values of \bar{Z} , compared with those of found in FIG. 1 (a) and (b). In this figure, we use a gap of value ~ 0.26 eV which is reported in single layer graphene due to SiC substrate by Zhou et al²¹, and we choose $M = 0.1t$ which corresponds to 270 meV with hopping energy $t = 2.7$ eV. Curves for

$$\bar{E}_n(M_0, \bar{Z}) = M_0 \text{sgn}(\bar{Z}) \left\{ 1 + \frac{\bar{Z}^2}{\left[n + \sqrt{(m+1/2)^2 - \bar{Z}^2} \right]^2} \right\}^{-1/2} \quad (15)$$

without magnetic field but with impurity³⁰, and curves for $\bar{E}_n^{\mp}(M_0, B) = \mp \sqrt{M_0^2 + (2n/\ell^2)}$ with magnetic field but without impurity are also plotted in the same figure for comparison purposes. Here, sgn is the sign function. We represent the former group, i.e., electron and hole energy bands, by horizontal solid lines, while the bold straight lines are used for the later one. We first notice that, with inclusion of gap/"mass" term, the behavior of the ground-state energy changes from a square root of B dependence to a linear dependence on B . As B is decreased, the curves for electron energies with $\bar{Z} = -0.1$ and -0.2 , and the curves for the hole energies with $\bar{Z} = 0.1$ and 0.2 , all they approach $\bar{E}_n(M_0, \bar{Z})$ indicated by horizontal lines which correspond to impurity energy in the absence of magnetic field. It should also be noted that, while the curve for gapped-graphene electron (hole) energy with $\bar{Z} = 0.05$ (-0.05) spreads very little through the gap, the curve for gapped-graphene electron (hole) energy with $\bar{Z} = 0.2$ (-0.1) lies significantly below the gap.

To understand this picture better, it is necessary to study the impurity binding energy, which is a measure of how much of \bar{E}_n^{\pm} consists of the charged Coulomb impurity. In other words, it is defined as the energy difference between the energy of graphene (massless or massive) without impurity and the energy of graphene with impurity,

i.e., $\Delta \overline{E}_n^{\pm BE} = \pm \sqrt{M_0^2 + (2n/\ell^2)} - \overline{E}_n^{\pm}$. In FIG. 3(a-c), impurity binding energies for low-lying gapless and gapped-graphene states are given for three different values of magnetic field strength. From these figures, we see that enhancement in magnetic field strength leads to more binding. Moreover, in the absence of gap term, binding energies for electrons (thin lines) and holes (thin dashed lines) have the same magnitude, i.e., they are all equal in magnitude under $\overline{Z} \rightarrow -\overline{Z}$.

To investigate the influence of gap/"mass" term in detail, we have also examined the dependence of \overline{Z}_{cr} on both magnetic field strength B and gap/mass term M_0 , in FIG. 4(a) and (b), respectively. The curves of the figure corresponds to \overline{E}_1^+ case only, since tendencies of changing of \overline{E}_1^- with B and M_0 are similar to those of \overline{E}_1^+ . For a given value of M_0 , as B is increased, the minimum value of \overline{Z}_{cr} curves shifts to larger values. As expected, all figures in FIG. 4(a) and (b) illustrate that, as \overline{M}_0 approaches to zero, threshold value of \overline{Z}_{cr} is given by 0.752 as is calculated above. By switching a gap, \overline{Z}_{cr} is drastically reduced compared to that found in the massless limit.

In FIG. 5(a) and (b) for comparison purposes, we plotted the evolution of \overline{Z}_{cr} as a function of (νm) for massless and massive cases, respectively. The energy levels are dependent on the principal quantum number n , and they are degenerate with respect to m , $-m$ and s . By comparing the left and right panels of FIG. 5(a), we see that the degeneracy of energy levels with respect to m , $-m$ are partially removed by the impurity. However, inclusion of a gap/"mass" term (FIG. 5(b)) splits the degeneracy of these levels with respect to m , $-m$ and s . Additionally, by switching a gap/"mass" term, we see that critical values of \overline{Z} are (i) smaller than those presented for the massless limit, and (ii) they diminish when increases for $(\nu, m < 0, +)$ while \overline{Z}_{cr} for $(\nu, m < 0, -)$ states increases. These are due to the fact that, while the massless Dirac-Weyl Hamiltonian with external fields commutes with helicity operator, i.e., it is invariant under the chiral transformation, the mass term is not, therefore it breaks the chiral symmetry. For the physical origin of this axial anomaly, we refer to the book of Huang³¹ where a detailed discussion of nonexistence of conserved axial vector current is given in a whole chapter, and we also refer to the paper of Lee *et al*³² wherein they concluded that first chiral states does not decouple, even in the massless limit, and second massless spinor electrodynamics is a pathological theory and therefore it should always be considered to be the limit of a massive theory.

In conclusion, we have investigated the effect of charged Coulomb impurity on the Landau level spectrum of both gapless and gapped-graphene near the Fermi point, by using their 2D continuum massless and massive Dirac descriptions, respectively, in the framework of a variational procedure. Since, we know that the success of variational treatment strongly depends on the choice of trial wave functions together with the set of parameters included, we suggest the basis sets of unperturbed Hamiltonian as trial wave functions with one parameter so as to reproduce the exact analytical results in the absence of perturbation. Indeed, to test the results of our variational calculation, it is enough to look at the change of variational parameter as a function of impurity strength Z . In the limit $Z \rightarrow 0$, the variational parameter becomes $\gamma = 1/\ell$. This is an indication of the adequacy of the trial wave function, since it yields the exact results in the absence of impurity, as expected. Furthermore, in the absence of impurity the variational parameter $\gamma = 1/\ell$ is the inverse order of magnitude of magnetic confinement length. When impurity is switched on, renormalization of the magnetic confinement length should be taken into account so as to adapt itself to the response of the presence of impurity, for which the energy develops a new minimum. This is achieved by adjusting the variational envelope wave function with a variational parameter γ until the energy is minimized. Thus, the inverse of γ may be interpreted as the amount of effective displacement of the magnetic confinement length caused by the impurity. Although the results of variational calculation we use give good agreement with the exact ones in the absence of impurity, and they also yield exact analytical results for the ground- and excited-states in the presence of impurity, such a description may not be accurate for the Landau bands with high indices in the case of high magnetic fields. In this case, adjacent Landau bands may overlap. As a consequence, a more sophisticated trial wave function composed of linear superpositions of trial wave functions we use with more than one variational parameter may be needed for a numerical approach.³³

In summary, by employing a variational procedure based on a choice of trial wave functions as the basis sets of Landau levels, we obtained analytical results for both energy eigenvalues and the critical Coulomb coupling strength as functions of both magnetic field strength and gap parameter for a graphene electron subjected to a homogeneous magnetic field in the presence of a charged Coulomb impurity. The analytical results that we obtained here show that (i) the critical impurity strength is independent of the magnetic field strength in the massless limit, and (ii) it drastically reduces when a gap/"mass" term is switched on. However, enhancement in magnetic field strength leads to increase in critical Coulomb coupling strength.

Acknowledgments

The authors thank Professor T. Altanhan for valuable discussions, and for a critically reading of the manuscript.

-
- ¹ K. S. Novoselov, A. K. Geim, S. V. Morozov, D. Jiang, Y. Zhang, S. V. Dubonos, I. V. Grigorieva, and A. A. Firsov, *Science* **306**, 666 (2004); K. S. Novoselov, D. Jiang, F. Schedin, T. J. Booth, V. V. Khotkevich, S. V. Morozov, and A. K. Geim, *Proc. Natl. Acad. Sci. USA* **102**, 10451 (2005).
 - ² A. K. Geim and K. S. Novoselov, *Nature Materials* **6**, 183 (2007); K. S. Novoselov, A. K. Geim, S. V. Morozov, D. Jiang, M. I. Katsnelson, I. V. Grigorieva, S. V. Dubonos, and A. A. Firsov, *Nature (London)* **438**, 197 (2005); Yuanbo Zhang, Yan-Wen Tan, Horst L. Stormer, and Philip Kim, *Nature* **438**, 201 (2005).
 - ³ P. R. Wallace, *Phys. Rev.* **71**, 622 (1947).
 - ⁴ Gordon W. Semenoff, *Phys. Rev. Lett.* **53**, 2449 (1984).
 - ⁵ P. M. Ostrovsky, I. V. Gornyi, and A. D. Mirlin, *Phys. Rev. B.* **74**, 235443 (2006).
 - ⁶ M. I. Katsnelson, *Phys. Rev. B.* **74**, 201401 (R) (2006).
 - ⁷ Vitor M. Pereira, Johan Nilsson, and A. H. Castro Neto, *Phys. Rev. Lett.* **99**, 166802 (2007).
 - ⁸ M. M. Fogler, D. S. Novikov, and B. I. Shklovskii, *Phys. Rev. B.* **76**, 233402 (2007).
 - ⁹ Ivan S. Terekhov, Alexander I. Milstein, Valeri N. Kotov, and Oleg P. Sushkov, *Phys. Rev. Lett.* **100**, 076803 (2008).
 - ¹⁰ Valeri N. Kotov, Vitor M. Pereira, and Bruno Uchoa, *Phys. Rev. B.* **78**, 075433 (2008).
 - ¹¹ Wei Zhu, Zhengfei Wang, Qinwei Shi, K. Y. Szeto, Jie Chen, and J. G. Hou, *Phys. Rev. B.* **79**, 155430 (2009).
 - ¹² Vitor M. Pereira, Valeri N. Kotov, and A. H. Castro Neto, *Phys. Rev. B.* **78**, 085101 (2008).
 - ¹³ D. P. DiVincenzo and E. J. Mele, *Phys. Rev. B.* **29**, 1685 (1984).
 - ¹⁴ J.-H. Chen, C. Jang, S. Adam, M. S. Fuhrer, E. D. Williams, and M. Ishigami, *Nature Phys.* **4**, 377 (2008).
 - ¹⁵ A. V. Shytov, M. I. Katsnelson, and L. S. Levitov, *Phys. Rev. Lett.* **99**, 236801 (2007).
 - ¹⁶ A. V. Shytov, M. I. Katsnelson, and L. S. Levitov, *Phys. Rev. Lett.* **99**, 246802 (2007).
 - ¹⁷ D. S. Novikov, *Appl. Phys. Lett.* **91**, 102102 (2007).
 - ¹⁸ D. S. Novikov, *Phys. Rev. B.* **76**, 245435 (2007).
 - ¹⁹ M. I. Katsnelson and A. K. Geim, *Phil. Trans. R. Soc. A* **366**, 195 (2008).
 - ²⁰ W. Greiner, B. Müller, and J. Rafelski, *Quantum Electrodynamics of Strong Fields* (Springer-Verlag Berlin Heidelberg, 1985).
 - ²¹ S. Y. Zhou, G.-H. Gweon, A. V. Fedorov, P. N. First, W. A. de Heer, D.-H. Lee, F. Guinea, A. H. Castro Neto, and A. Lanzara, *Nature Materials* **6**, 770 (2007).
 - ²² C. L. Kane and E. J. Mele, *Phys. Rev. Lett.* **95**, 226801 (2005).

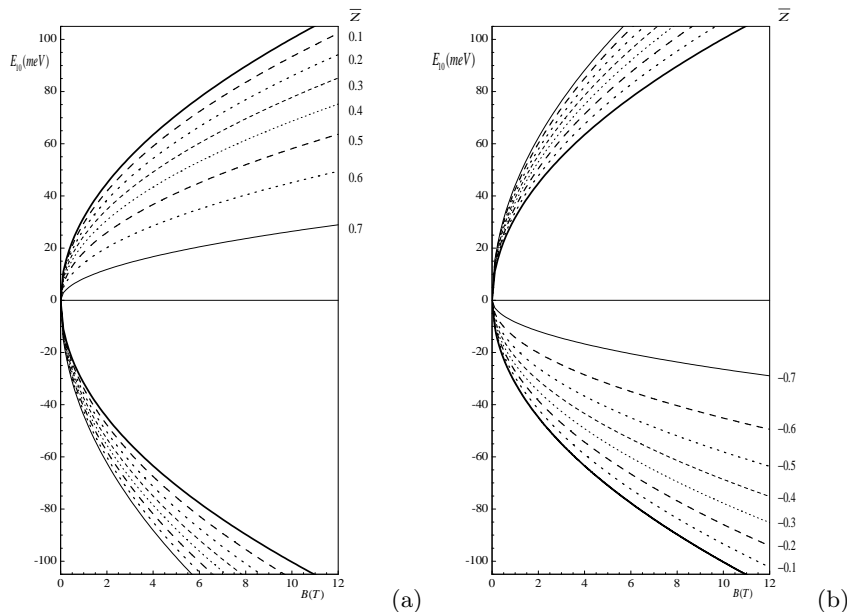


FIG. 1: (a) Plots of the lowest (i.e., $n = 1$ corresponding to the levels $(\nu, m, s) = (0, 1, -1)$, and $(0, 0, +1)$) Landau energy $\overline{E}_1^{(\pm)}$ of gapless graphene electron and hole, calculated by Eq. (12) as a function of magnetic field for various positive values of \overline{Z} . (b) Same as (a), but for negative values of \overline{Z} .

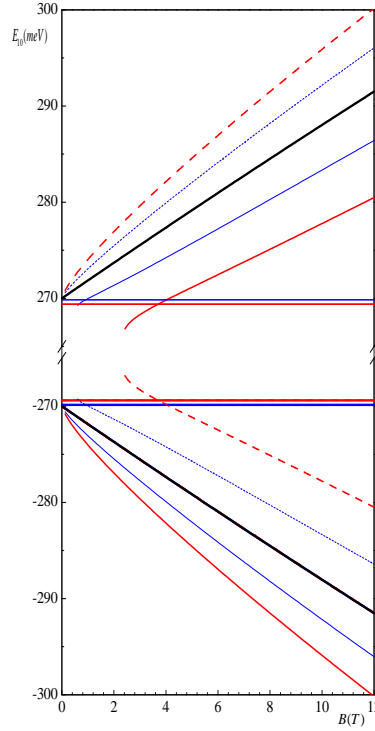


FIG. 2: (Color online) Dependence of the lowest Landau Level of the gapped graphene on magnetic field, calculated by Eq. (12). While the thin and thick dashed curves mark $\bar{Z} = -0.05$ and $\bar{Z} = -0.1$, respectively, the thin and thick solid lines mark $\bar{Z} = 0.05$ and $\bar{Z} = 0.1$, respectively. The thick bold lines corresponds unperturbed $\bar{E}_1^\pm = \pm\sqrt{M_0^2 + (2/\ell^2)}$ energy levels, i.e., in the absence of impurity, graphene electron and hole ground-state energies, respectively. The horizontal solid lines refer to the associated impurity eigenvalues in the absence of magnetic field, i.e., Eq. (15) with $n = 1, m = 0$.

- ²³ K. Nakada, M. Fujita, G. Dresselhaus, and M. S. Dresselhaus, Phys. Rev. B. **54**, 17954 (1996); Young-Woo Son, Marvin L. Cohen, and Steven G. Louie, Phys. Rev. Lett. **97**, 216803 (2006); *ibid*, Phys. Rev. Lett. **98**, 089901 (E) (2007); Melinda Y. Han, Barbaros Özyilmaz, Yuanbo Zhang, and Philip Kim, Phys. Rev. Lett. **98**, 206805 (2007).
- ²⁴ Choon-Lin Ho and V. R. Khalilov, Phys. Rev. A. **61**, 032104 (2000).
- ²⁵ Alexander Turbinger, Phys. Rev. A. **50**, 5335 (1994).
- ²⁶ B. S. Kandemir, J. Math. Phys. **46**, 032110 (2005); *ibid*, Phys. Rev. B. **72**, 165350 (2005).
- ²⁷ Kaushik Bhattacharya, arXiv:0705.4275v2 [hep-th] (2007).
- ²⁸ I. S. Gradshteyn and I. M. Ryzhik, *Table of Integrals, Series and Products* (Academic Press, New York, 6th edition, 2000).
- ²⁹ D. Griffiths, *Introduction to Elementary Particles* (John Wiley and Sons, New York, 1987).
- ³⁰ W. Greiner, *Relativistic Quantum Mechanics* (Springer-Verlag Berlin Heidelberg, 1994).
- ³¹ Kerson Huang, *Quarks, Leptons and Gauge Fields* (World Scientific, Singapore, 1982).
- ³² T. D. Lee and M. Nauenberg, Phys.Rev. **133**, B1549 (1964).
- ³³ B. S. Kandemir and A. Mogulkoc, Eur. Phys. J. B DOI: 10.1140/epjb/e2010-00051-4 (2010).

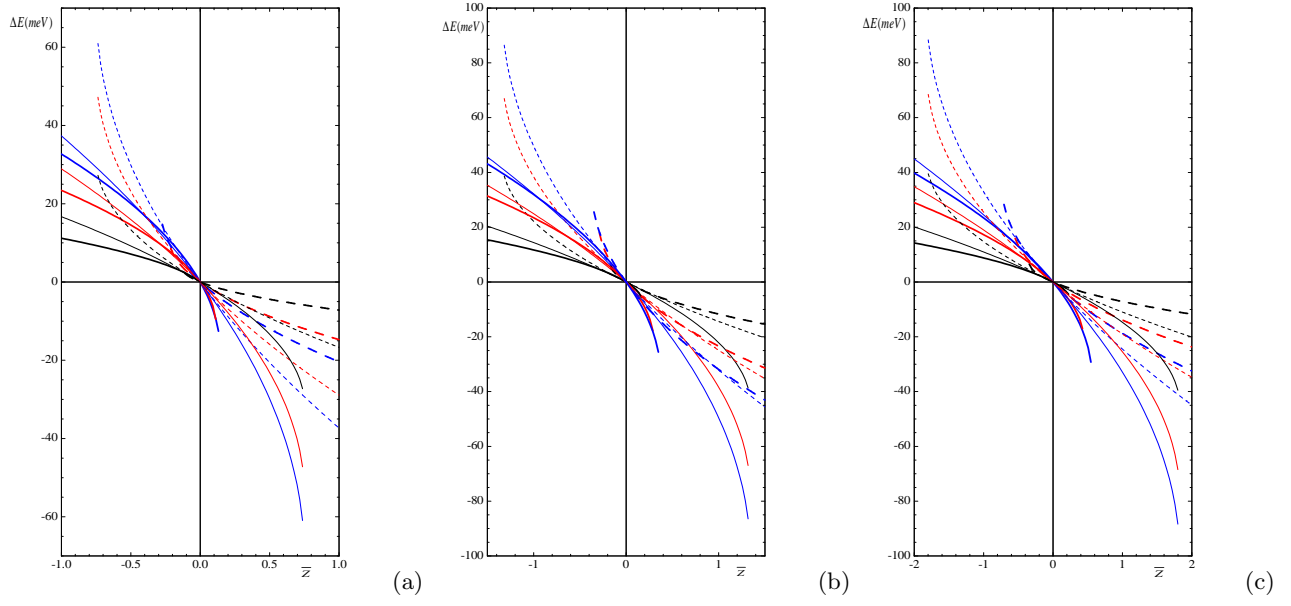


FIG. 3: (Color online) Impurity binding energies of gapless graphene electron (thin solid lines) and gapless graphene hole (thin dashed lines) as a function of \bar{z} for the three low-lying Landau levels, i.e., (a) for (10), (b) for (20), (c) for (21), for three values of magnetic field, $B = 1$ (black), 3 (red) and 5T (blue). Binding energies of gapped graphene electron and hole states are also shown in the same graphs but by thick counterparts for $\bar{M}_0 = M_0/t = 0.1$.

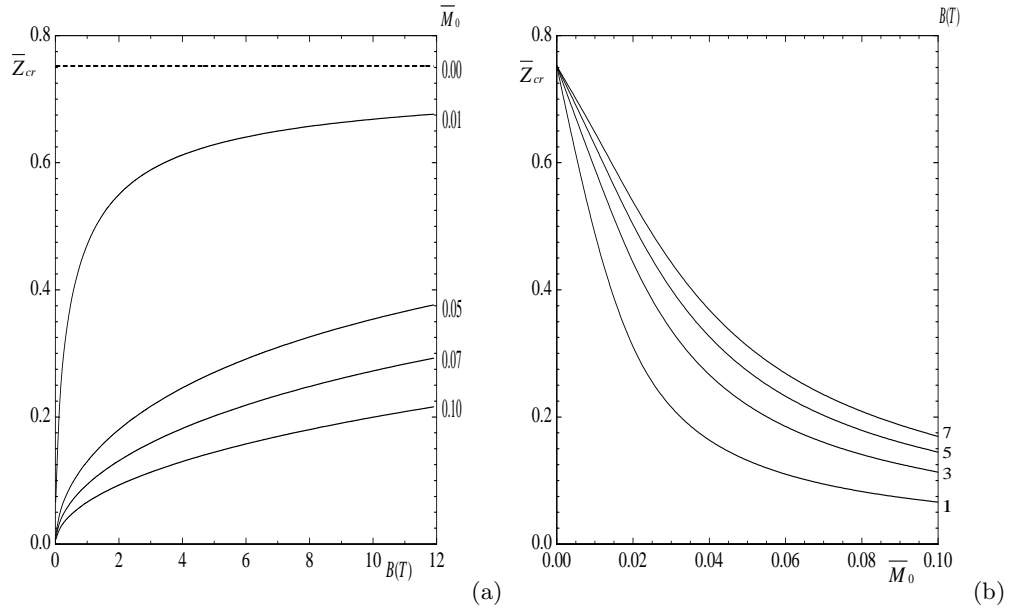


FIG. 4: (a) The critical value of \bar{z}_{cr} given by Eq. (13) as a function of magnetic field for four different gap values, and (b) as a function of gap parameter, but for four different magnetic field values.

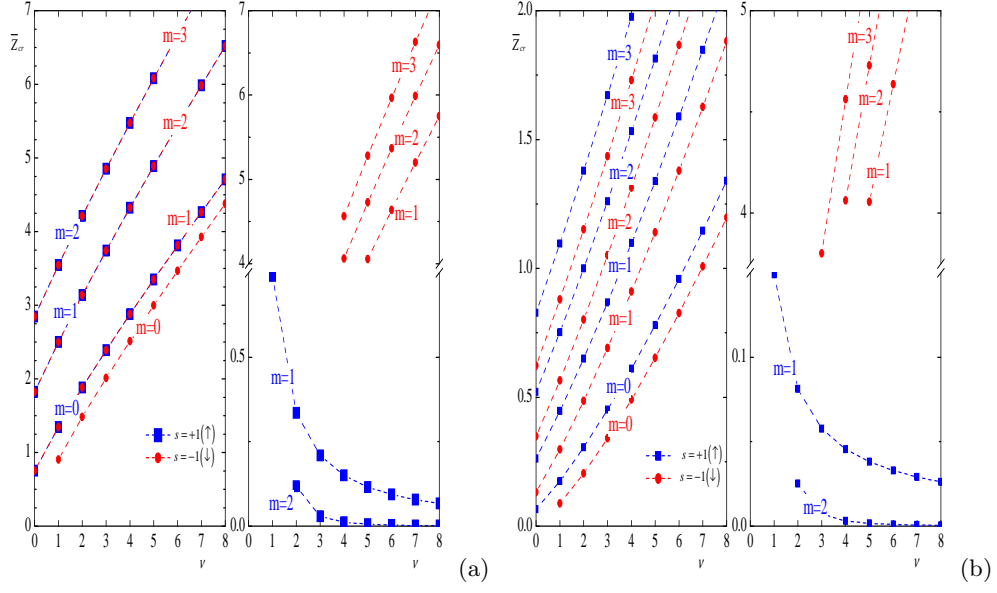


FIG. 5: (Color online) Dependence of the critical value of Coulomb coupling strength, i.e., \bar{Z}_{cr} on quantum numbers (νm) for (a) without gap, $\bar{M}_0 = 0$ (b) with gap, $\bar{M}_0 = 0, 1$, respectively. The dashed lines are drawn to guide the eye. In these figures, left panels corresponds to $m \geq 0$, while the right ones refer to $m < 0$.